Journal of Power Sources 196 (2011) 10550–10555

Contents lists available at SciVerse ScienceDirect

Journal of Power Sources

journal homepage: www.elsevier.com/locate/jpowsour

Oxygen activation over engineered surface grains on YDC/YSZ interlayered composite electrolyte for LT-SOFC

Young Beom Kim[a,*,1], Joong Sun Park[a,1], Turgut M. Gür[b], Fritz B. Prinz[a,b]

[a] Department of Mechanical Engineering, Stanford University, Stanford, CA 94305, USA
[b] Department of Material Science and Engineering, Stanford University, Stanford, CA 94305, USA

ARTICLE INFO

Article history:
Received 1 July 2011
Received in revised form 17 August 2011
Accepted 18 August 2011
Available online 31 August 2011

Keywords:
Yttria-doped ceria
Low-temperature SOFC
Cathodic interlayer
YDC/YSZ composite electrolyte
YDC surface grain boundary activity
Oxygen kinetics

ABSTRACT

This paper reports the role of surface grain boundaries in enhancing oxygen incorporation kinetics on oxide ion conducting yttria-doped ceria (YDC) ceramic electrolyte. Thin YDC interlayered (~400 nm) YSZ composite electrolyte was successfully fabricated by pulsed laser deposition (PLD) on the cathode side of 100 μm-thick polycrystalline substrate. Oxygen isotope exchange experiment was conducted employing secondary ion mass spectrometry (SIMS) with high spatial resolution (50 nm). Surface mapping result of $^{18}O/^{16}O$ shows that high activity at surface grain boundary regions indicating that the grain boundary regions are electrochemically active for oxygen incorporation reaction. In addition, fuel cell current–voltage measurements and electrochemical impedance spectroscopy study were performed in the temperature range of 350–450 °C on surface-engineered electrode-membrane assemblies (MEA) having different YDC surface grain sizes. Results from both dc and ac measurements confirm again that fuel cell MEAs having smaller surface grain size show better performance than large grain surfaces. Up to 4-fold increase was observed in power density and correspondingly lower electrode interface resistance. The collective results of SIMS and electrochemical measurements indicate that the YDC grain boundary regions at the cathode side are electrochemically active for oxygen surface kinetics. The results of this study provide an opportunity and incentive for designing high performing LT-SOFCs by surface engineering of YSZ electrolyte with nano-granular, catalytically superior thin YDC cathodic interlayers.

1. Introduction

Solid oxide fuel cells (SOFCs) have long been investigated for efficient and environmental friendly energy conversion. They typically employ yttria stabilized zirconia (YSZ) solid electrolyte due to its selective oxide ion conductivity, superior chemical stability, and wide electrolytic domain that expands over several decades of oxygen activity. However, high activation energy (~1 eV) for ionic transport in YSZ necessitates operation usually at high temperatures (800–1000 °C). This temperature regime poses challenges in materials selection, compatibility, stability, and cost that limit materials options. It is therefore desirable to reduce the operating temperature of SOFCs to lower than 500 °C [1,2]. Unfortunately, in this low temperature regime, two critical factors become much more pronounced and adversely affect the performance of low-temperature SOFCs (LT-SOFC). One is increased ohmic resistance due to slower ionic transport through the YSZ electrolyte at these temperatures. The other is similarly increased activation losses mostly due to slower kinetics of the oxygen reduction reaction at the cathode [1,2].

These adverse effects can be mitigated by the use of doped ceria based materials for LT-SOFCs. Indeed, acceptor doped cerium oxides such as gadolinia doped ceria (GDC) and yttria doped ceria (YDC) have higher ionic conductivity than YSZ below 700 °C. Therefore, ceria based electrolytes are proposed for intermediate temperature (500–700 °C) solid oxide fuel cell applications [3–5]. It is also suggested by Steele that the surface exchange coefficient has a positive relationship with oxygen diffusivity in the material [6]. Indeed, doped cerium oxides are known to be good oxidation catalysts due to higher surface exchange coefficients that lead to several times faster kinetics for oxygen reduction at the triple phase boundary (TPB) than YSZ in the intermediate temperature regime [7–10]. However, chemical stability of doped cerium oxides is compromised in reducing environments where ensuing electronic conductivity leads to inferior cell performance. To fully utilize the advantages of doped cerium oxides and avoid instability

* Corresponding author at: 440 Escondido Mall, Bldg. 530 Rm. 226, Stanford, CA 94305, USA. Tel.: +1 650 796 5957; fax: +1 650 723 5034.
E-mail address: ybkim@stanford.edu (Y.B. Kim).
[1] These authors contributed equally to this work.

0378-7753/$ – see front matter © 2011 Elsevier B.V. All rights reserved.
doi:10.1016/j.jpowsour.2011.08.075

issues, many research groups have fabricated and studied composite electrolytes composed of doped ceria in combination of a stable oxygen ion conductor such as YSZ [11–17].

Previous work in our laboratory had indicated that inserting nanoscale thin GDC interlayer at the cathode side of the YSZ substrate significantly enhanced fuel cell performance by reducing the activation loss associated with oxygen reduction reaction (ORR) at the cathode [18,19]. Similarly, others theoretically observed low activation overpotentials with thin cathodes and ionic conducting YSZ electrolyte with small grain sizes [16,20,21]. We hypothesized in this paper that the nanogranular structure of doped cerium oxide surface was largely responsible for the performance enhancement in these studies. Accordingly, we investigated the contribution of grain size and hence, the surface grain boundaries of doped cerium oxides in improving the cathode kinetics of ORR.

In this study, we present spectrometric and spectroscopic evidence indicating enhanced activity at surface grain boundaries. We demonstrate successful fabrication of interlayered YDC/YSZ composite electrolyte by employing pulsed laser deposition (PLD) technique. By controlling post-annealing temperatures, we have systematically varied the size of surface grains of YDC interlayer deposited on the cathode side. In addition, we present the results of fuel cell performance and how they are affected by the size of YDC surface grains, i.e., the grain boundary density on the YDC external surface at the cathode side. The cell performance was characterized by current–voltage measurements in the temperature range of 350–450 °C while cathode interfacial resistances were extracted from electrochemical impedance data. Moreover, the calculated exchange current density values are also in support of the above experimental data. The findings of this paper provide important implications for engineering the cathode surface grain structure of YDC/YSZ composite electrolytes in order to enhance fuel cell performance.

2. Experimental

Experiments were done on two types of sample categories. The first category involved surface microstructure and oxygen exchange measurements on commercial (Japan Fine Ceramics) sintered YDC pellets 1 cm × 1 cm in size and 500 μm in thickness. The second category of experiments involved fuel cell and electrode impedance studies as a function of YDC surface grain size (i.e., grain boundary density) on composite electrolyte samples having a thin YDC layer deposited on the cathode sides of YSZ substrates.

The surface microstructure of commercially available YDC pellets was analyzed by FEI XL30 Sirion scanning electron microscopy (SEM). These pellets were also employed for oxygen isotope exchange experiments, where incorporation was carried under DC biased conditions applied across porous platinum cathode and anode layers sputtered on both faces of the 500 μm-thick polycrystalline YDC pellets. Isotope exchange experiments involved evacuation of the vessel to at least 10^{-6} Torr followed by the introduction of research grade (>99%) $^{18}O_2$ gas at 150 ± 1 Torr, which is equivalent to the ambient oxygen partial pressure. The YDC samples were annealed at 400 °C for 3 hours in $^{18}O_2$ under 1 V of externally applied cathodic (negative) bias. Prior to $^{18}O_2$ exchange, the samples were annealed in 150 Torr of $^{16}O_2$ environment for at least three times the isotope exchange time.^{18}O and ^{16}O ion counts were measured simultaneously by using high spatial resolution SIMS (NanoSIMS-50L, Cameca, France). A primary Cs^+ ion beam (16 keV) was applied to analyze the secondary ions emitted from the samples. As the primary ion beam sputters the surface (10 μm × 10 μm of rastered area and 256 × 256 pixel with dwell time of 1 ms/pixel), the concentration of ions was measured layer by layer as a function of depth.

The second category of experiments employed cells with layered YDC/YSZ composite electrolyte, which were fabricated by pulsed laser deposition (PLD) technique. 100 μm-thick polycrystalline YSZ wafers (1 cm × 1 cm, BEANS International Corp.) were used for bottom substrates. A sintered 10-mol percent yttria doped cerium oxide pellet (Kurt J. Lesker) was used as a target to deposit thin YDC films on one face of the YSZ wafers, that would then become the cathode side. The YSZ substrate temperature was maintained at 750 °C during deposition. A Lambda Physik 248 nm KrF excimer laser with energy density of 1.5 J cm^{-2} per pulse was used for ablating the target in 100mTorr background oxygen gas environment in the deposition chamber. The sample-to-target distance was maintained at 50 mm during deposition and about 400 nm of YDC layer was deposited on YSZ at a rate of ~0.22 Å per pulse.

After deposition, the samples were post annealed at various temperatures between 750 °C and 1500 °C in ambient air for 10 h to obtain different grain size samples in the YDC layers. The size of YDC grains on the surface was measured by atomic force microscopy (AFM) (XE-70 Park Systems Inc.) operated in non-contact surface scanning mode. 80 nm of porous Pt catalytic electrodes were deposited on both sides by DC sputtering technique under 50 W of plasma power and 10 Pa of Ar pressure for 150 s at room temperature.

For fuel cell performance measurements, we used a customized micro-probing test station developed earlier in our laboratory [19]. The gas-tight chamber is mounted on a heat controlled station to maintain constant temperature. During measurements, pure hydrogen was supplied at the anode side while the cathode side is exposed to ambient air. For the acquisition of fuel cell polarization behavior and electrochemical impedance spectroscopy (EIS) data, a Gamry Potentiostat (FAS2, Gamry Instruments, Inc.) unit was used. Fuel cell performance was measured at temperatures from 350–450 °C and EIS was measured under various fuel cell voltage conditions in the frequency range from 300 kHz down to 0.1 Hz. ZView software (Scribner Associate, Inc.) was used to analyze the EIS spectra based on complex nonlinear least-squares fitting [22].

3. Results and discussion

3.1. Oxygen exchange measurements with YDC sintered pellets

Fig. 1(a) shows the SEM of the microstructure and topography of the polycrystalline YDC pellet surface, indicating an average grain size of 6 + 1 μm. Sintered polycrystalline YDC pellets were also employed in oxygen exchange experiments conducted under a cathodic DC bias of 1 V while annealing in $^{18}O_2$ environment at 400 °C. Surface activity for ORR was determined by the use of a high spatial resolution SIMS (NanoSIMS) with a beam size less than 100 nm. The NanoSIMS image presented in Fig. 1(b) as the $^{18}O/^{16}O$ ratio clearly indicates enhanced activity along the grain boundary regions on the YDC surface. The $^{18}O/^{16}O$ count ratio in grain boundary regions are about two times higher than that in bulk regions at this operation condition. This result agrees well with previous work and observations in our laboratory on YSZ surfaces, and confirming that this phenomenon is not unique to YSZ [23]. It also provides spectrometric evidence that grain boundaries on the external surfaces of ionic conducting oxides provide preferential sites for oxygen incorporation, possibly due to higher concentration of vacancies in the grain boundary region [24].

3.2. Size-engineered surface grains on YDC/YSZ composite electrolyte

To study how grain size affects electrochemical behavior, YDC films were fabricated with size-engineered surface grains

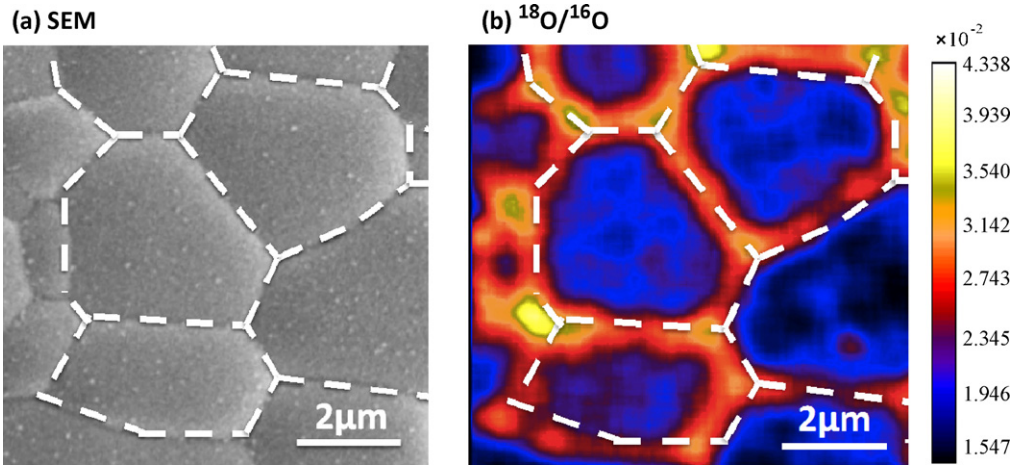

Fig. 1. (a) Surface SEM image of YDC sintered pellet, where dashed line shows clear grain boundaries. (b) $^{18}O/^{16}O$ concentration map of corresponding YDC surface obtained from NanoSIMS, where the scale bar shows the relative concentration of ^{18}O to ^{16}O counts. The $^{18}O/^{16}O$ count ratio is significantly higher at grain boundary regions (dashed) than the grain surface regions indicating a larger population of oxygen isotopes in the grain boundary regions.

at the cathode sides of the fuel cell elements. Size engineering of grains was achieved by controlling the post annealing temperature for these films. YDC surface microstructure of YDC/YSZ samples was determined by AFM. Fig. 2 shows the AFM topography images of YDC surfaces after post-annealing at temperatures from 750 °C to 1500 °C. As expected, lower annealing temperatures yield smaller grain size in the sub-micrometer regime, namely, 55 ± 15 nm for 750 °C (Fig. 2(a)) and 120 ± 30 nm

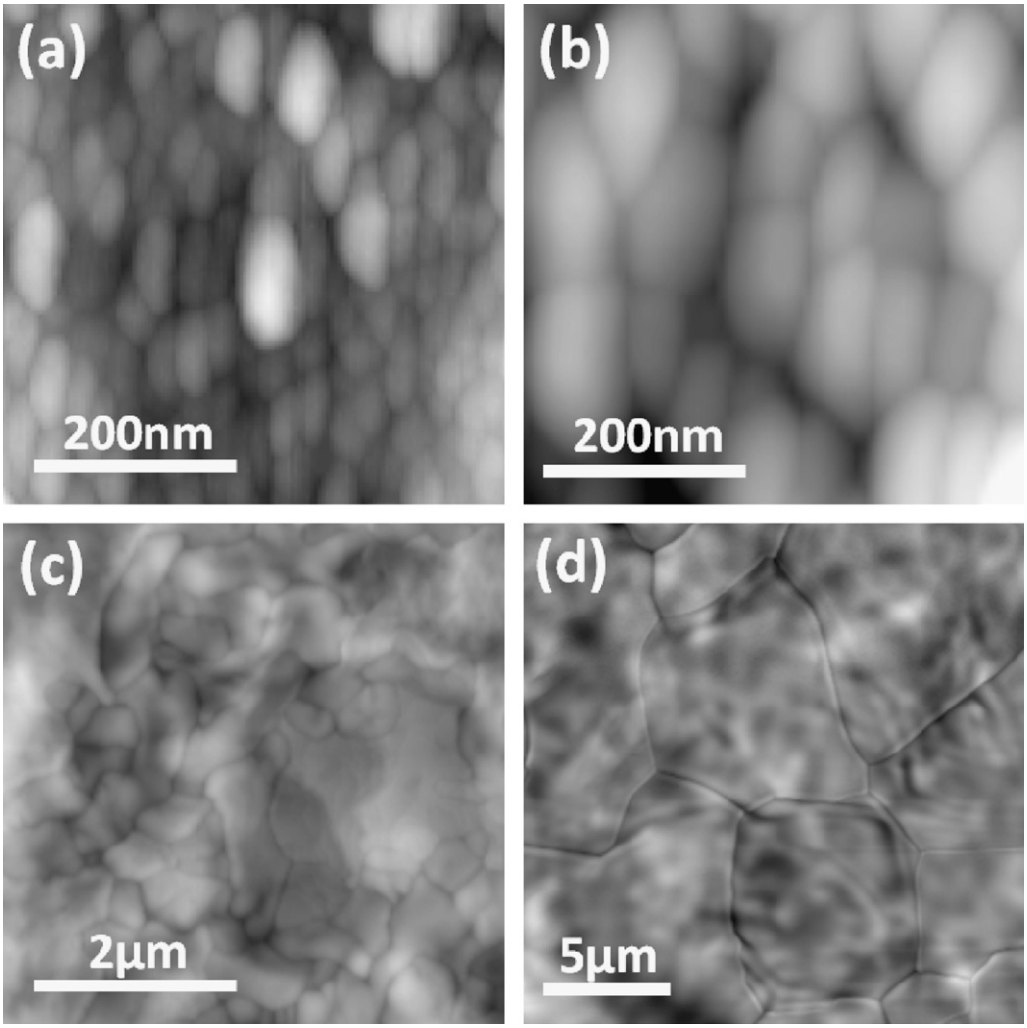

Fig. 2. AFM images of YDC surface additionally deposited on polycrystalline YSZ substrate and post-annealed at different temperatures. (a) 750 °C, (b) 1100 °C, (c) 1300 °C, and (d) 1500 °C.

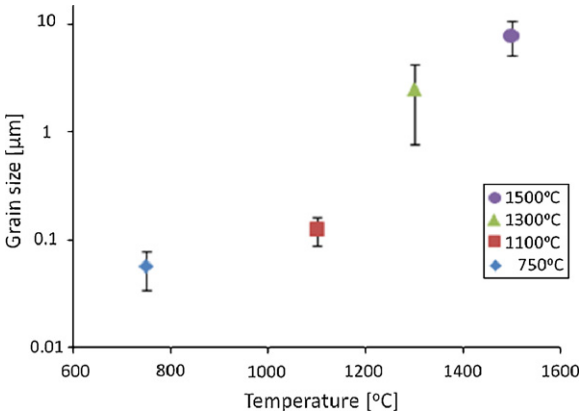

Fig. 3. Average grain size of YDC interlayer as a function of post-annealing temperature.

for the 1100 °C (Fig. 2(b)) samples. Higher annealing temperatures result in grain sizes 2.02 ± 1.04 μm for the 1300 °C sample (Fig. 2(c)) and 6.50 ± 1.72 μm for the 1500 °C sample (Fig. 2(d)), respectively. Fig. 3 shows the resulting average grain sizes as a function of annealing temperature. This post annealing process affects grain growth only in the thin YDC interlayer, but has no significant effect on the grain size and microstructure of the underlying YSZ substrate. In other words, the grain size of only the cathode interface has been varied in these experiments while the grain size at bulk and the anode interface remained practically unchanged. This was confirmed by our previous experiments using PLD YSZ thin interlayers in our laboratory [23]. Therefore any significant variations in the electrochemical behavior of these samples can be associated with the role of grain size at the cathode interface.

The first set of experimental evidence supporting the role of grain size comes from fuel cell measurements. After deposition of porous Pt electrodes on both sides of these samples under identical sputtering conditions, their fuel cell performances were measured at temperatures from 350 °C to 450 °C using hydrogen as the fuel and air as the oxidant. Open circuit voltage (OCV) values were in the range of 1.03–1.06 V vs air for all measured samples. Fig. 4 shows the current–voltage (*I*–*V*) behavior of YDC/YSZ composite SOFC samples measured at 400 °C with varied grain sizes (or, grain boundary densities) at the cathode side. The data show consistent improvement in the fuel cell performance with decreasing grain size at the YDC surface. Indeed, the composite sample with the smallest grain size at the YDC surface that corresponds to the

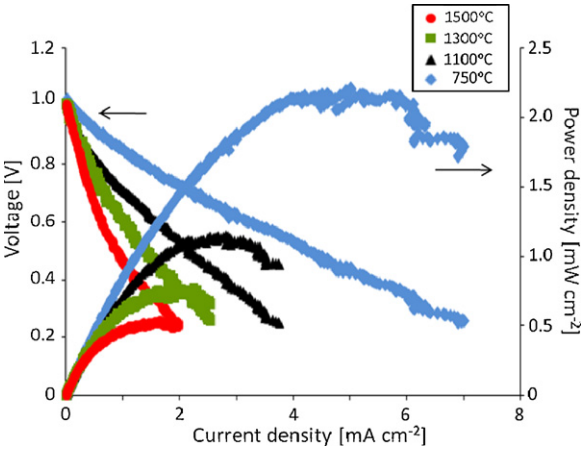

Fig. 4. Current–voltage (*I*–*V*) behavior of fuel cell MEAs measured at 400 °C. Fuel cells with smaller surface grain size show higher performance in terms of peak power densities.

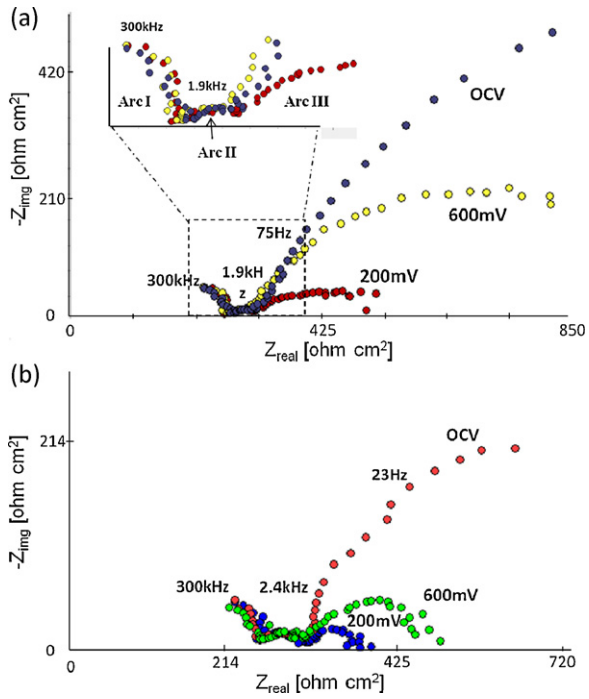

Fig. 5. Electrochemical impedance spectroscopy (EIS) data of (a) 1500 °C and (b) 750 °C annealed YDC/YSZ composite fuel cell sample measured at 350 °C indicating three loops. The two high frequency loops seem to be independent of cell voltage conditions, indicating that these arcs correspond to ionic transport through electrolyte and representing bulk (arc I) and grain boundary (arc II). whereas the low frequency loop shows dependence on cell voltage conditions indicating that this arc corresponds to the electrode interface resistance.

highest grain boundary density also shows the highest peak power density and the lowest activation loss. In other words, having more grain boundaries at the cathode interface significantly enhanced the fuel cell performance in terms of peak power density by up to 4-fold and this enhancement is primarily due to improved cathode activation for the oxygen reduction reaction.

In order to exclude the possibility of surface roughness effects contributing to increased fuel cell performance, the average roughness of YDC surface was measured by AFM for all samples. We measured multiple spots for each sample and found the root mean square (RMS) roughness value was about 4–20 nm. Based on our previous experimental results, the contribution from such roughness values to the effective surface area is rather marginal, with an estimated enhancement of only 1–3%. Therefore, one can exclude surface area effects and conclude that the improvement in fuel cell performance with decreasing grain size is primarily due to enhanced oxygen reduction kinetics, which is consistent with SIMS results of Fig. 1, and not from an increase in the effective reaction site density due to surface roughness.

The second set of experimental evidence supporting the role of grain size (i.e., surface grain boundary density) comes from electrochemical impedance spectroscopy (EIS) measurements. Accordingly, the effect of the YDC grain boundary density at the cathode side was studied by EIS for each sample at different temperatures. Fig. 5 shows a representative Nyquist plot for the 1500 °C post-annealed composite sample measured at 350 °C under various cell voltage conditions. The spectra indicates three arcs, where the two high frequency arcs (arc I and arc II) showed no discernible change under three different cell voltage conditions indicating that these two arcs are most likely associated with ionic transport across bulk grains and grain boundaries, respectively [5]. The total electrolyte resistance value, which is sum of the two high frequency arcs, matches well with the reference conductivity value for YSZ at

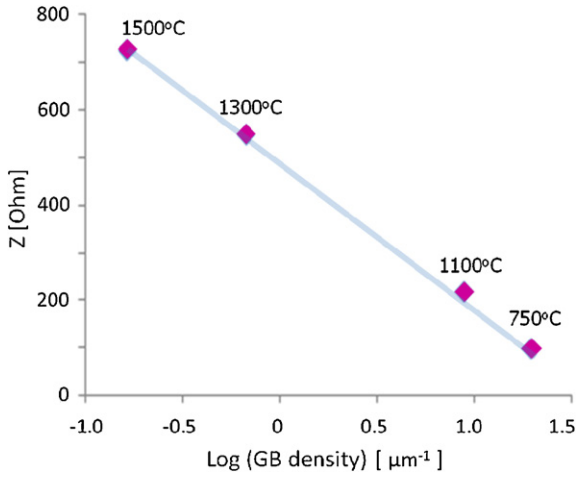

Fig. 6. A plot showing extracted electrode interface resistances (at 450 °C, 0.6 V) as a function of estimated surface grain boundary densities. As expected, the electrode resistance decreases as the surface grain boundary density increases (lower grain sizes).

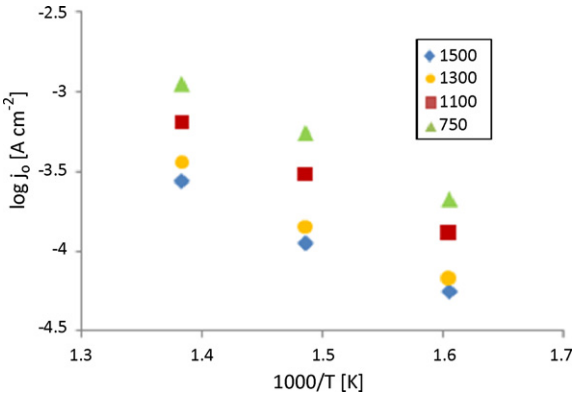

Fig. 7. Exchange current densities for all measured samples with different grain sizes were calculated at temperatures 350–50 °C. As the surface grain size decreases (i.e., higher grain boundary density), the electrode interface resistance decreases. This indicates that the surface grain boundaries enhance oxygen surface kinetics at the cathode side.

the measured temperature [25,26]. Possible increase in electrolyte resistance due to the additional thin YDC layer can be neglected since its contribution is merely 0.1% of the ohmic resistance of YSZ under this experimental condition. The ionic conductivity of YDC is more than an order of magnitude higher than that of YSZ at this temperature, and the thickness of added YDC interlayer is almost three orders of magnitude smaller than the thickness of the YSZ substrate. Thus, it can be assumed that ohmic resistance is primarily due to the YSZ bulk substrate. This is also confirmed by recent experiments in our laboratory [27]. In contrast, the low frequency arc is highly affected by the cell voltage conditions suggesting that this arc corresponds to electrode processes, most likely associated with the cathode reaction as discussed previously.

By using a representative equivalent circuit model, the values for electrolyte and electrode (cathode) resistances are extracted for all measured samples. Representative electrode interface resistance values (450 °C at 0.6 V cell voltage condition) are plotted in Fig. 6 as a function of surface grain boundary (GB) density estimated from values in Fig. 3. Grain boundary density is experimentally determined from SEM images of YDC surfaces and defined as total grain boundary length per unit area. As expected, the electrode resistance decreases with increasing surface grain boundary density. This clearly indicates that the YDC surface grain boundary enhances the oxygen exchange rate at the cathode surface. Qualitatively, the semilog dependence depicted in Fig. 6 is to be expected since impedance directly relates to the resulting overvoltage, which in turn exhibits a semilog dependence to current through the Butler–Volmer relationship. In addition, exchange current densities (j_0), which relate to the charge transfer reaction rate at the cathode, were calculated from EIS and *I–V* data. From the measured *I–V* fuel cell performances, the exchange current density (j_0) was extrapolated by fitting the activation or polarization loss (η_{act}) and current density (j) values to the Tafel approximation [28]:

$$\eta_{act} = \frac{RT}{\alpha nF} \ln \frac{j}{j_0} \quad (1)$$

where R is the ideal gas constant, α is the charge transfer coefficient, n is the number of electrons involved in the electrode interface reaction, and F is the Faradic constant. Fig. 7 shows the results for all the YDC/YSZ composite samples measured in the temperature regime of 350–450 °C and indicates activation energies of 0.62–0.66 eV. The composite 1500 °C annealed sample having the largest grain size (5–7 μm), i.e., the lowest density of surface grain boundaries, has shown the lowest exchange current density values. It is consistently observed that cathodic interface resistances of the samples decrease as the grain size of the YDC interlayer decreases by lowering the post-annealing temperature. The resistance values for the nano-grain size sample (40–70 nm) which was annealed at the deposition temperature of 750 °C showed the lowest resistance values, about 6–7-fold less compared to that of the largest grain sample, at each measurement temperature. Results in Fig. 7 and the EIS analysis indicate that the exchange current density as well as the cathodic interface resistance scales with grain size, more precisely, the grain boundary density on the YDC surface. Smaller surface grains naturally generate higher grain boundary density at the cathode interface. The fuel cell MEA with higher YDC surface grain boundary density (i.e.,smaller grain size) shows higher exchange current densities. This study clearly demonstrates that such nanogranular surface microstructure gives rise to higher charge transfer rate at the cathode side. Based collectively on the results presented in this paper, we postulate that surface grain boundaries serve as active sites for enhanced oxygen exchange kinetics.

Enhanced fuel cell performance by improving oxygen reduction kinetics on nanoscale thin doped-cerium oxide was previously observed in our laboratory. Huang et al. demonstrated enhanced cell performance by adopting nano-crystalline GDC thin film at the cathode side of the YSZ composite.[18] Simulation results by H.B. Lee et al. utilizing molecular dynamics (MD) demonstrated segregation of oxygen vacancies in gadolinia doped ceria (GDC) to surface grain boundary regions [29]. Accordingly, we postulate that increased presence of vacancies in the grain boundary regions promote ORR. Also, Lee et al. experimentally confirmed the segregation of oxygen vacancies to grain boundaries on external surfaces by measuring surface potential distribution on GDC surfaces by using conductive AFM technique [30]. They reported a comparative study between surface topography and the corresponding surface potential map of the same imaged region. It indicated a more positive surface potential at surface grain boundaries that was likely due to the segregation of positively charged oxygen vacancies to these regions, whereas bulk grain surfaces exhibited lower positive potentials.

We speculate that these results that were obtained for GDC also holds true for the case of YDC as well, opening up opportunities to surface engineer LT-SOFCs for improved performance.

4. Conclusion

The effect of YDC surface grain size and grain boundary density on fuel cell performance was investigated using spectrometric, spectroscopic and electrochemical measurements. Surface

mapping of ^{18}O and ^{16}O ions by a high spatial resolution NanoSIMS indicated preferential enrichment of ^{18}O along grain boundaries on the YDC external surface. The YDC/YSZ composite structure was fabricated by adding a thin YDC layer on the cathode side of the bulk polycrystalline YSZ substrate (100 μm-thick). The grain size at the cathode side was systematically varied over a wide range (from 40–70 nm to 5–7 μm) by controlling the post-annealing temperature from 750 °C to 1500 °C. The sizes of surface grains were measured by AFM topography for each sample. The fuel cell performances measured in the temperature range from 350 °C to 450 °C correlated well with the YDC surface grain size, where best performance was obtained for the smallest grain size, i.e., the highest surface grain boundary density, and vice versa. AC impedance spectroscopy, also measured in the temperature range from 350 °C to 450 °C, indicated significantly lower cathodic interfacial resistances for smaller surface grain sizes. Moreover, the exchange current densities were calculated and showed similar trend that higher surface grain boundary density results the higher charge transfer rate. This suggests that smaller surface grains facilitate enhancement in oxygen reduction kinetics.

This study successfully demonstrated the significant effect of surface grain size on reducing cathodic interface resistance as well as improving fuel cell performance. Results of this study provide significant implications in designing nano-granular YDC surfaces to achieve enhanced LT-SOFC performance by improving oxygen surface kinetics.

Acknowledgments

T.M.G. and F.B.P. gratefully acknowledge partial support from the Center on Nanostructuring for Efficient Energy Conversion (CNEEC) at Stanford University, an Energy Frontier Research Center funded by the U.S. Department of Energy, Office of Science, Office of Basic Energy Sciences under Award Number DE-SC0001060. This research used resources of the National Energy Research Scientific Computing Center, which is supported by the Office of Science of the U.S. Department of Energy under Contract No. DE-AC02-05CH11231. J.S.P. was partially supported by Samsung Scholarship.

References

[1] B.C.H. Steele, A. Heinzel, Nature 414 (2001) 345–352.
[2] N.P. Brandon, S. Skinner, B.C.H. Steele, Annu. Rev. Mater. Res. 33 (2003) 183–213.
[3] B.C.H. Steele, Solid State Ionics 129 (2000) 95.
[4] J.A. Kilner, Solid State Ionics 129 (2000) 13–23.
[5] H.L. Tuller, Solid State Ionics 131 (2000) 143–157.
[6] B.C.H. Steele, Solid State Ionics 75 (1995) 157–165.
[7] T. Hibino, A. Hashimoto, T. Inoue, J. Tokuno, S. Yoshina, M. Sano, Science 288 (2000) 2031.
[8] H. Uchida, M. Yoshida, M. Watanabe, J. Phys. Chem. 99 (1995) 3282.
[9] B.C.H. Steele, K.M. Hori, S. Uchino, Solid State Ionics 135 (2000) 445.
[10] J.A. Lane, J.A. Kilner, Solid State Ionics 136 (2000) 927–932.
[11] A.V. Virkar, J. Electrochem. Soc. 138 (1991) 1481–1487.
[12] F.M.B. Marques, L.M. Navarro, Solid State Ionics 90 (1996) 183–192.
[13] H. Yahiro, Y. Baba, K. Eguchi, H. Arai, J. Electrochem. Soc. 135 (1988) 2077–2080.
[14] K. Eguchi, T. Setoguchi, T. Inoue, H. Arai, Solid State Ionics 52 (1992) 165–172.
[15] K. Mehta, S.J. Hong, J.F. Jue, A.V. Virkar, S.C. Singhal, H. Iwahara (Eds.), Proceedings of the 3rd International Symposium on Solid Oxide Fuel Cells, Electrochemical Society, Pennington, NJ, 1997, pp. 92–103.
[16] T. Tsai, S.A. Barnett, Solid State Ionics 98 (1997) 191–196.
[17] S.G. Kim, S.P. Yoon, S.W. Nam, S.H. Hyun, S.A. Hong, J. Power Sources 110 (2002) 222–228.
[18] H. Huang, T. Holme, F.B. Prinz, J. Fuel Cell Sci. Technol. 7 (2010) 1–5.
[19] H. Huang, M. Nakamura, P.C. Su, R. Fasching, Y. Saito, F.B. Prinz, J. Electrochem. Soc. 154 (2007) B20–B24.
[20] C.W. Tanner, K.Z. Fung, A.V. Virkar, J. Electrochem. Soc. 144 (1997) 21–30.
[21] S.H. Chan, X.J. Chen, K.A. Khor, J. Electrochem. Soc. 151 (2004) A164–A172.
[22] E. Barsoukov, J.R. Macdonald, Impedance Spectroscopy: Theory, Experiment and Applications, 2nd ed., Wiley, New York, 2005.
[23] J. Shim, J. Park, T. Holme, K. Crabb, W. Lee, Y.B. Kim, X. Tian, T.M. Gür, F.B. Prinz, Acta Mater. (submitted for publication).
[24] W. Lee, M. Lee, H.-J. Jung, F.B. Prinz, Meet. Abstr. Electrochem. Soc. 1001 (2010) 724.
[25] S.M. Haile, Acta Mater. 51 (2003) 5981–6000.
[26] B.C.H. Steele, Mater. Sci. Eng. 79 (2002) B13.
[27] Y.B. Kim, T. Holme, T.M. Gür, F.B. Prinz, Adv. Func. Mater., in press, doi:10.1002/adfm.20110105.
[28] A.J. Bard, L.R. Faulkner, Electrochemical Methods, 2nd ed., John Wiley & Sons, New York, 2001.
[29] H.B. Lee, F.B. Prinz, W. Cai, Acta Mater. 58 (2010) 2197–2206.
[30] M. Lee, W. Lee, F.B. Prinz, Nanotechnology 17 (2006) 3728–3733.